Research Article

Comparative Analysis of Swirl Burner and Cross Jet Burner in Terms of Efficiency and Environmental Performance

Mikhail G. Zhumagulov [1], **Maxim V. Dolgov** [2], **Askar A. Baubek** [1], and **Alexander M. Gribkov** [3]

[1]*NC Eurasian National University, Faculty of Transport and Power Engineering, Astana 010000, Kazakhstan*
[2]*Thermal Power Engineering, NC Eurasian National University, Faculty of Transport and Power Engineering, Astana 010000, Kazakhstan*
[3]*Kazan State Energy University, Kazan 420000, Tatarstan, Russia*

Correspondence should be addressed to Maxim V. Dolgov; maxwellhousebest@yandex.ru

The article contains a comparative analysis of two types of burners used in different methods of fuel-air mixture preparation: (1) vortex mixing and (2) mixing with transverse jets. The analysis was carried out in order to determine which one of the two burning devices is more efficient and has better environmental performance. In device no. 1, conditions for the fuel-air mixture formation are created by vortex turbulence. The basic principle lying at the core of this design is a vortex flow inside, which provokes a more intense mixing of fuel and air. Moreover, preliminary physical and thermal treatment of the fuel-air mixture has a positive effect on its environmental performance. In contrast, in device no. 2 based on transverse jets' active mixture formation is achieved through collision of air and fuel flows at an angle close to 90°. The research was based on an experiment carried out with the use of a laboratory firing stand. Flue gas samples were analyzed in order to compare the main harmful air emission indicators with TESTO 350-XL gas analyzer. A propane-butane mixture of 60% C_3H_8 (propane) and 40% C_4H_{10} (butane) was used as the main fuel. Some indicators were determined after the experiment: measurement units conversion from "ppm" to "mg/m^3," excess air ratio α and equivalence ratio φ, flue gas concentrations recalculation taking oxygen into account, fuel calorific value, and heat release rate. The analysis results are as follows: (i) the swirl burner shows better performance in terms of nitrogen oxides (NO_x) emissions; there is a 1.75-fold difference in total NO_x emissions compared to the cross jet burner; (ii) the burner on transverse jets is 10 times more efficient than the swirl burner in terms of carbon monoxide (CO) emissions.

1. Introduction

Humanity's fossil fuel burning technology has reached tangible heights. Most modern burners are capable of burning known design fuels with efficiency level above 92%. New issues arise as modern combustion devices become increasingly sophisticated and new operating conditions are formed. This marked the beginning of competition for fractions of a percent of efficiency. In terms of environmental performance, the situation is roughly the same. Emission levels have been reduced to an attainable minimum. All further attempts to reduce emissions have

insignificant success. In order to stimulate progress in this area, countries adopt legislations to lower emission thresholds. For example, the CIS Interstate Standard [1] provides that "the nitrogen oxides content shall not exceed 150 mg/m^3 (73.17 ppm) for a gas turbine plant without regeneration and 200 mg/m^3 (97.56 ppm) for a gas turbine plant with heat regeneration (in exhaust gases at 0°C, 0.1013 MPa, and reference oxygen concentration of 15%)" and "carbon monoxide content in exhaust gases shall not exceed 300 mg/m^3 (240 ppm)." The US EPA (Environmental Protection Agency, USA) standards are the most stringent –205 mg/m^3 (100 ppm) of nitrogen oxide emissions for

equipment with a capacity up to 3.5 MW. As the capacity increases to 110 MW and more, the emission threshold decreases to 30 mg/m^3 (15 ppm) [2]. The maximum carbon monoxide emission is set at 63 mg/m^3 (50 ppm) [3]. It also depends on the equipment installed capacity. The European Union directive [4] sets medium environmental requirements: NO$_x$ 50 mg/m^3 (24 ppm) and CO 100 mg/m^3 (80 ppm) for natural gas; NO$_x$ 120 mg/m^3 (60 ppm) and CO 100 mg/m^3 (80 ppm) for other gas types. Similar emission standard was adopted in China in 2020 [5]. According to the standard, average concentrations of NO$_x$ emissions during combustion should not exceed 150 mg/m^3 (73.17 ppm).

A rich variety of burner devices have been developed by science and technology so far, featuring high efficiency and permissible level of harmful emissions into the environment. For example, the medium-capacity power boilers mostly use universal burners without premixing to flare high-calorific low- or high-pressure natural gas [6]. In external mixing burners, the active mixing zone is localized at the base of flame to ensure a stable combustion process. This is characteristic of any of the many burner designs, especially those which aim to create a vortex or jet ejection enhancing the heat and mass transfer [7]. In contrast to the described devices, burners with premixing [8] allow significant reduction of harmful emissions without loss of combustion efficiency of gaseous and, in some cases, liquid fuels, provided they are mainly used in combustion chambers of gas turbines. The most commonly used device of this kind is lean premixed prevaporized burner [9], which has a great potential for carbon monoxide (CO) and nitrogen oxide (NO$_x$) emissions reduction [10–12]. It provides a homogeneous lean mixture of air and fuel that can burn at lower temperatures thus reducing thermal NO$_x$ emissions. However, the key feature of lean mixture combustion is its sensitivity to external disturbances resulting in flame stabilization problems [13–15] or thermo-acoustic instabilities [16, 17]. The device is greatly limited to certain types of fuel and fields of application.

An alternative device is the porous burner that has shown excellent performance in terms of low emission levels, high combustion stability, increased power density, and the ability to operate at ultralow combustion rates [18]. One of the disadvantages of this design is limited maximum heat output. It is therefore not studied further in this research. Another promising area of development is turbulent flows creation by separated (transverse) jets. Eventually, harmful emissions reduction can be observed [19, 20]. In [21], the effect of jet inclination on mixing processes compared to transverse flow was studied using the turbulence model. The effect of using axial fuel injection with variable orifices in swirl burners was investigated for flashback resistance [22]. Flashback resistance optimization is achieved through increase in the diameter of axial fuel jet contributing to vortex displacement [23]. Although axial fuel injection along the centerline has been shown to have a wider performance, the technique can result in significantly higher NO$_x$ emissions [24] due to localization of high temperature zones. The use of central air injection is

a suitable alternative to central fuel injection in terms of NO$_x$ emissions reduction, where distributed reaction conditions in the combustion chamber can be achieved through air injection rate control [25].

The flameless combustion regime is also well known, which delivered on the promise of ultralow NO$_x$ and CO emissions levels. However, the high temperatures of the stoichiometric flames would produce the greatest NO$_x$ emissions [26].

Unlike other methods, MILD (moderate or intense low oxygen dilution) combustion produces a much more uniform temperature distribution with a lower peak value. MILD combustion has larger CO production rate than traditional combustion and generates a higher CO peak value in the reaction zone [27]. MILD combustion regime was achieved for a wide range of external parameters with reduced combustion peak temperatures and very low NO$_x$ and CO emissions in a wide operational window. Scaling the combustor at higher heat intensity renders the system very complex and makes its implementation highly challenging [28].

A large amount of central air injection can increase flashback resistance and significantly reduce NO$_x$ volumes [29]. Thus, the practice of initial fuel and air injection into the preignition chamber has every chance to prove effective.

The authors of the theoretical study [30] propose a method for reducing the formation of NO$_x$ by organizing fuel zoning and diffusion combustion; that is, gas fuel is mixed with part of the heated air, and then the products of incomplete combustion diffusely burn in the rest of air. This principle allowed them to reduce nitrogen oxides to 312.89 mg/m^3 (152.6 ppm) according to the computer simulation data. The transfer of this principle from the heat flue in a coke oven to burners for various purposes can lead to a positive result, especially if it is experimentally verified. This idea is taken into account by the authors of the present article in the burner device no. 1 in an adapted version.

Xu et al. [31] describe an equipment which adopts a self-circulation method to reduce harmful NO$_x$ emissions. It allows them to significantly reduce nitrogen oxides by limitation of the oxygen concentration and temperature in the combustion zone. The recommendation by [32] ratio of flue gas (circulation) to air is 0.6, which made it possible to reduce NO$_x$ to 128.42 mg/m^3 (62.64 ppm) and prevent significant CO emissions. Circulation is provided by using the energy within a high-pressure motive fluid (gas fuel or air) to entrain a low-pressure suction fluid (flue gas) to an intermediate discharge pressure (ejector effect). This theoretical study notes that low velocities of parallel fuel and air flows do not provide the necessary mixing of fuel and air. In addition, the high pressure of the motive fluid is the main condition for the existence of self-circulation, which is associated with the need for a compressor or other high-power supercharger. It can complicate and increase the cost of the burner. As an alternative, the vortex is able to achieve efficient mixing using lower linear velocities, since high vortex velocities are created by swirling, as is carried out in the burner device no. 1 of the present research.

The studies described above are summarized as follows:

(1) Efficient mixing of fuel and air is necessary to reduce CO emissions, that is, to increase the thermal efficiency of combustion. It is carried out in

    (a) vortex flow due to the intensity of turbulence [8]
    (b) cross jets due to collision of flows [19]
    (c) parallel jets due to the speed or pressure of fluid [31]

(2) It is necessary for reducing NOx emissions,

    (a) reducing the temperature in local areas by mixing with rest of air [9]
    (b) distributing the flame over the volume of the combustion chamber [18]
    (c) circulation of flue gas into the chamber space [31]

Two different designs of burners were created within the scope of this research. They work on the basis of different methods of fuel-air mixture preparation: (1) vortex mixing and (2) mixing with cross jets. Parallel jets are not considered according to [31]. The two methods are compared in terms of their efficiency and environmental performance, and the newly created burner devices have the aim to provide efficient combustion with low harmful emissions of NO_x and CO.

The authors of this article have made previous attempts to create a universal burner device in terms of fuel selection (prototype of device no. 1) [33].

Vortex turbulence is known to create favorable conditions for fuel-air mixture formation [34]. Reynolds number is considered to be the main indicator of turbulence. The basic principle lying at the core of this design is the vortex flow inside, which provokes a more intense mixing of fuel and air. Experiments [35] have shown that physical and thermal pretreatment of fuel-air mixture has a positive effect on its environmental performance due to the uniform distribution of the flame in the burner space with a moderate swirling. As an alternative to vortex turbulence technology, employees of the Kazan State Power Engineering University (Kazan, Tatarstan) developed the design of a burner with transverse jets (device no. 2) where active mixing is achieved through collision of air and fuel flows at an angle close to 90°. Effective environmental performance of this device is achieved by breaking up local high temperature zones with cross jets. The design is simpler in execution and operation, all flows are direct, but unlike device no. 1, device no. 2 is only suitable for combustion of gaseous fuel.

This paper provides comparison of the two combustion principles: vortex combustion and transverse jet combustion. The relevant burner devices were tested on a special stand in order to determine harmful NO_x and CO emissions. The propane-butane mixture is representative of LPG (liquified petroleum gas) mixtures that widely used a different scale of operation. LPG has a wide variety of uses in many different markets.

2. Materials and Methods

2.1. Object of Study. The study focused on the combustion process in two fundamentally different burner designs. The dimensions of both units were designed to ensure the same fuel consumption.

2.1.1. Device No. 1. The swirl burner device [36, 37] works similar to the cyclone boiler by Babcock and Wilcox [38], the difference being that the fuel and air inlet into prechamber 1 (Figure 1) is not axial but tangential. This type of feed is known to create intensive swirling flow inside the chamber. Fuel and air are fed through inlets 2 and 3 and begin to actively mix and react in chamber 1. Vortex is actively generated in chamber 1 in the form of a mini tornado with deep rarefaction created on the axis. Low pressure contributes to fuel involvement (suction) in circulation and fuel-air medium release into the outlet nozzle 4. Nozzle 4 has a recess inside chamber 1, which helps to reduce the flow aerodynamic resistance at the outlet from chamber 1 due to "soft" friction of the gaseous medium against itself rather than against the chamber wall.

Device no. 1 was originally designed as a universal burner, which is capable of burning various liquid and gaseous fuels without significant modifications to the design (Figure 2). The versatility and unpretentiousness of the burner in relation to the type of fuel is one of the main advantages of the unit.

2.1.2. Device No. 2. The cross jet burner is based on the principle of fuel and air flows collision at an angle close to 90°, which facilitates active mixing. The jet trajectory depends on momentum ratio between the two streams.

The device (Figure 3) consists of two main parts: the stationary part (flange) 2, bolted to the combustion chamber 6, and the movable part 1, sliding on the stationary part in axial direction and moved by device 4.

There are holes on the inner wall of the movable part 1 for air access, 4 mm in diameter, arranged in a staggered pattern. Changing the burner position relative to the flange makes the passage area larger or smaller, and consequently the speed of transverse air jets changes at a constant flow rate, since part of the holes is blocked by the flange and the output speed through the remaining "open" holes either increases or decreases. This, in turn, changes the mixing and combustion process in the furnace.

Device no. 2 was designed as a burner, which is capable of burning gaseous fuels only (Figure 4).

2.2. Experimental. The experimental study of swirl burner and cross jet gas burner operation was carried out with the use of a laboratory firing stand in order to compare the main emission indicators through flue gas sample analysis with the TESTO 350-XL gas analyzer.
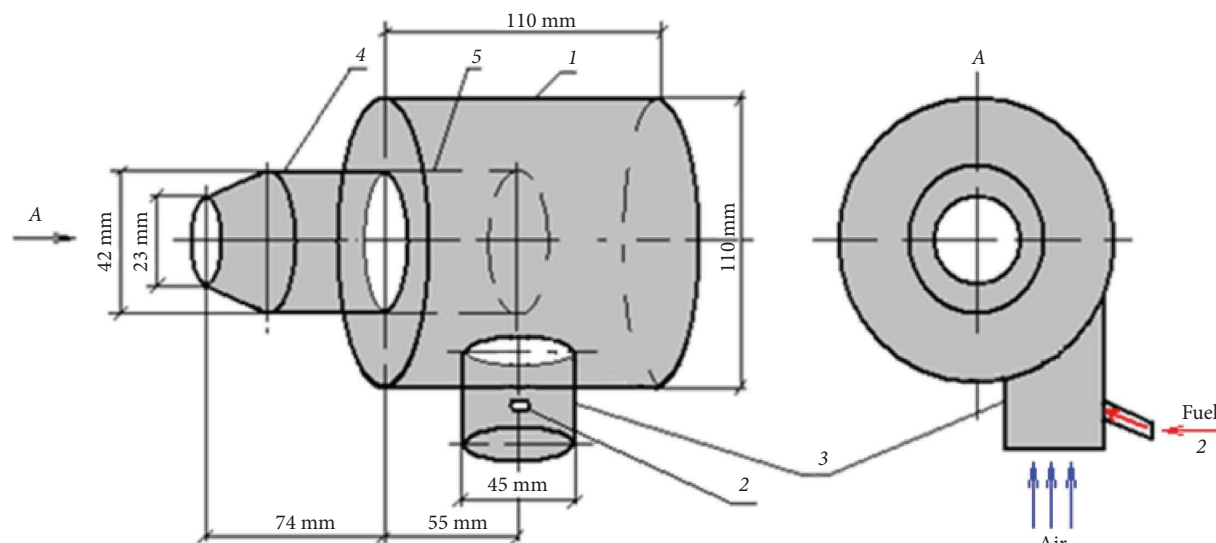
1 - Pre-mixing and ignition chamber; *2* - Fuel inlet connection;
3 - Air inlet connection; *4* - Exhaust connection; *5* - Exhaust connection protrusion

Figure 1: Swirl burner device.

Figure 2: Swirl burner device in operation.

A propane-butane mixture of 60% C_3H_8 (propane) and 40% C_4H_{10} (butane) was used as the main fuel which is the most readily available, predictable, and flammable.

The firing stand in Figure 5 enables analysis of the resulting combustion products under different gas burner operating conditions.

The main element of the firing stand is a gas-tight combustion chamber 1 where gaseous fuel supplied from cylinder 17 is combusted in the burner 2. Valve 20 is used for gas flow regulation. Combustion air is supplied by the air flow rate booster 13 regulated by the autotransformer 3. The flare is ignited through the igniter 5. Hatches 6 are provided for flare observation. Differential manometers 14 and 15 measure air and fuel consumption. Flue gas samples are collected through the hatch 21. Pump 24 is used to pump flue gas samples through the sampling line 22. The shut-off valve 23 controls the flue gas flow direction: to the pump and into the air or to the sampling probe of the gas analyzer. A millivoltmeter 10 is used to determine the flue gas temperature.

The flue gas temperature at the stand outlet was determined with an MR-64-02 millivoltmeter and a thermocouple. Type K thermocouple (Nickel-Chromium vs Nickel-

Aluminium) was used in the experiment. The permissible measurement deviation limit is ΔE; mV is calculated according to the following formula [39]:

$$\Delta E = 0.16 + 2 \cdot 10^{-4} \cdot (t - 300), \tag{1}$$

where t is the measuring temperature, °C.

At the temperature values obtained, the measurement limit was 0.16 mV, which corresponds to 4.03°C for a chromel-alumel thermocouple. The relative error is $\delta_t = 3.1\%$.

Millivoltmeter MR-64-02 is a panel profile instrument with a two-position regulating device of magneto-electric system. Millivoltmeter MR-64-02 is designed for operation at ambient temperature from +10°C to +35°C and relative humidity up to 80%. The basic permissible error of the millivoltmeter at all scale marks does not exceed $\delta_{mV} = 1.5\%$ [40].

The second part of the firing stand is the universal portable TESTO 350-XL measuring system, consisting of a control module, analyzer, and sampling probe. The measuring system is shown in Figure 6.

The TESTO 350-XL is used to collect and analyze flue gas samples obtained in the combustion chamber of the firing unit. The control module 2 (Figure 6) of the gas

1 - perforated cylinder; *2* - flange with seals; *3* - igniter opening; *4* - burner moving device;
5 - drive; *6* - combustion chamber front wall; *7* - burner flame
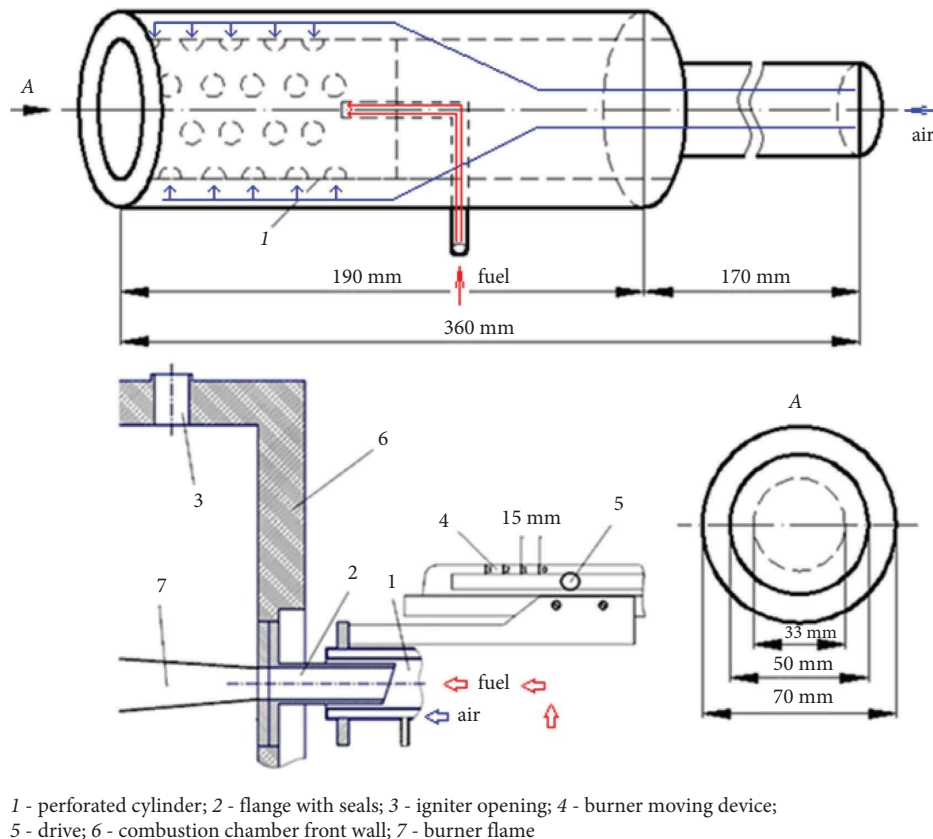
FIGURE 3: Gas burner with cross jet mixing.

FIGURE 4: Cross jet gas burner in operation.

analyzer displays measurement data and enables control of the device. The sampling probe 5 is used to take a gas sample and deliver it to the measuring device. The operating principle of the TESTO 350-XL is based on electrochemical measuring cells.

During the preliminary phase of the experiment, the TESTO 350-XL was calibrated in strict accordance with the manufacturer's instructions [41]. Without calibration before the experiment, it can lead to gross inaccuracies in measurements.

The measurement range of TESTO 350-XL is shown in Table 1.

The device draws flue gases in (flow rate of approx. 0.8 l/min) through the gas sampling probe using an integrated pump. After gas is cleaned and dried, it flows to the electrochemical cells. The measured parameters are continuously shown on the display: O_2, oxygen, %; CO, carbon

monoxide, ppm; NO_x, nitrogen oxides, ppm; and T_G, flue gas temperature, °C.

Flue gases flow from the combustion chamber into the gas discharge pipe with internal diameter $d = 130$ mm.

The experiment was carried out stepwise with two burner designs in order to compare the main indicators of flue gas samples.

(1) The fuel flow controller enabled three fuel flow settings:

  (i) 0.358 kg/h
  (ii) 0.438 kg/h
  (iii) 0.506 kg/h

(2) The air flow rate was set to achieve stable combustion. The oxidant content was gradually increased with air flow regulator, and several positions were measured for further graphic analysis. A 2-minute interval was maintained between measurements, during which a flue gas sample was pumped through the sampling line.

The estimate of the permissible error of the measuring system is calculated as the rms sum of the errors of the components of the measuring system:

$$\delta_{MS} = \sqrt{\delta_t^2 + \delta_{mV}^2 + \delta_{TESTO}^2},$$
$$\delta_{MS} = \sqrt{3.1^2 + 1.5^2 + 5^2} = 6.07\,\%. \tag{2}$$
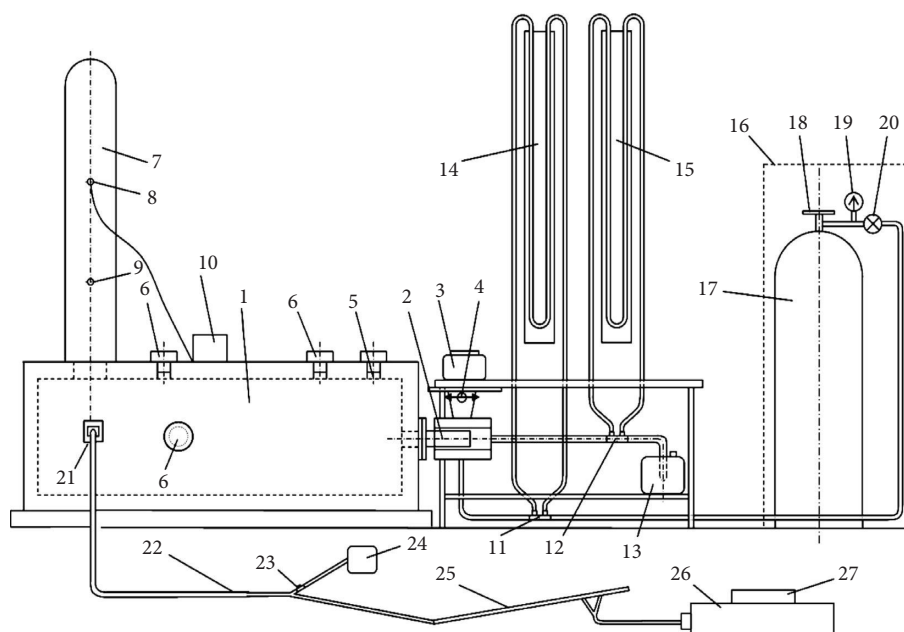
1 - combustion chamber; 2 - burner; 3 - autotransformer; 4 - device for burner moving;
5 - igniter; 6 - sight-holes; 7 - exhaust pipe; 8 - thermocouple; 9 - choke; 10 - millivoltmeter;
11, 12 - flow rate washers; 13 - air flow switch; 14, 15 - fuel and air flow differential manometers;
16 - corps; 17 - gas cylinder; 18 - stop valve; 19 - manometer; 20 - flow regulator; 21 - sampling hatch;
22 - sampling line; 23 - shut-off valve; 24 - sample pump; 25 - sampling probe; 26 - gas analyzer;
27 - control module

FIGURE 5: Firing stand.

1 - gas analyzer;

2 - control module;

3 - ON/OFF button;

4 - display;

5 - sampling probe

FIGURE 6: TESTO 350-XL measuring system.

For laboratory and semiindustrial emissions measurement experiments, the value of the relative error limit of the measuring system $\delta_{MS} = 6.07\%$ is considered acceptable.

TABLE 1: TESTO 350-XL measurement range.

Measurement value	Measurement range	Measurement error, δ_{TESTO} (%)
O_2	0–5%	±0.8
CO	0–10000 ppm	±5
NO	0–3000 ppm	±5
NO_2	0–500 ppm	±5

Each experiment was repeated 5 times. The relative statistical error of the measurement has been determined. The relative error of the measuring system does not exceed the permissible error.

2.3. Calculations

(1) Conversion from "ppm" to "mg/m³." The concentration unit commonly used in the entire range of TESTO gas analyzers is "ppm."

The ppm is the volumetric concentration, i.e., the number of molecules of a measured substance out of a million gas molecules and is independent of the temperature or pressure of the environment.

In order to compare the results of this experiment with similar research, "ppm" had to be converted to "mg/m³." NO_x and CO concentrations were converted from weight "mg/m³" to volumetric "ppm" dimension and vice versa using the following formulas:

$$C_{\mathrm{NO}x}(\mathrm{ppm}) = \frac{C_{\mathrm{NO}x}\left(\mathrm{mg}/m^3\right)}{2.05},$$

$$C_{\mathrm{CO}}(\mathrm{ppm}) = \frac{C_{\mathrm{CO}}\left(\mathrm{mg}/m^3\right)}{1.25}. \tag{3}$$

where 2.05 is the density of nitrogen dioxide under normal conditions, (kg/m^3);

1.25 is the density of carbon monoxide under normal conditions, (kg/m^3).

"NO_x" refers to a combination of NO, NO_2.

(2) Excess air ratio is defined as follows:

$$\alpha = \frac{G_a}{B_f \bullet G_o}, \tag{4}$$

where G_a is the actual airflow measured in the experiment (m_a^3/s);

B_f is the fuel consumption measured in the experiment (m_f^3/s);

G_o is the theoretical airflow rate (m_a^3/m_f^3):

$$\begin{aligned} G_o &= 0.0478 \bullet \left[\sum \left(m + \frac{n}{4} \right) \bullet C_m H_n \right] \\ &= 0,0478 \bullet \left[5 \bullet C_3 H_8 + 6,5 \bullet C_4 H_{10} \right], \end{aligned} \tag{5}$$

where C_3H_8 and C_4H_{10} are the volumetric concentrations of fuel components, %v.

Depending on the industry sector, the term "equivalence ratio φ" is often used in science instead of "excess air ratio." Equivalence ratio is the ratio of actual fuel/air ratio to stoichiometric fuel/air ratio. It is defined as follows:

$$\varphi = \frac{1}{\alpha}. \tag{6}$$

Both ratios are presented later in the figures together.

(3) Flue gas concentrations recalculation with oxygen. According to the oxygen formula, excess air ratio can be calculated as follows:

$$\alpha = \frac{21}{21 - O_2}, \tag{7}$$

where O_2 is the oxygen content in flue gases, %.

The normal (reference) value of O_2^r in swirl burners is 3%, which corresponds to an approximate value $\alpha = 1.17$ ($\varphi = 0.85$). In gas turbine combustion chambers, for example, the oxygen content in the combustion chambers of gas turbines is $O_2^r = 15\%$, which corresponds to $\alpha = 3.5$ ($\varphi = 0.29$) in excess air conditions. When harmful emissions were measured, NO_x and CO values were defined at the actual oxygen content in combustion products, which depends on the excess air ratio and combustion efficiency and is determined in the experiment.

Therefore, for emissions comparison, NO_x and CO values are converted to the reference oxygen content in combustion products O_2^r.

$$NO_x^r = NO_x^a \frac{(21 - O_2^r)}{21 - O_2^a}, \tag{8}$$

where NO_x^r is the reduced NOx concentration at oxygen content O_2^r, %;

NO_x^a is the measured (actual) concentration of the test gas;

O_2^a is the measured oxygen concentration in combustion products.

The carbon monoxide (CO) concentration in flue gases has been recalculated in a similar way.

(4) Determination of the Reynolds number. Reynolds number is the main indicator of turbulence intensity. Also, turbulence in turn directly influences the mixing efficiency of fuel and air [34]. Reynolds number is calculated by the following formula:

$$Re = \frac{v \bullet l}{\nu}, \tag{9}$$

where v is the gas flow velocity, m/s;

l is the characteristic size. The diameter applies to the pipe, m;

ν is the kinematic viscosity of the gas flow, m^2/s.

Let us calculate the Reynolds numbers for the two devices. Device 1 operates at Reynolds numbers $Re = 5809.19/7678.26$ (Table 2), while device 2 exhibits lower $Re = 1728.51/4697.66$ (Table 3). Obviously, device 1 has larger turbulence foci than device 2. As a consequence, mixing in unit 1 is more intense.

(5) Fuel calorific value. The lower fuel calorific value Q^d, MJ/m^3 was calculated using the following formula:

$$Q^d = 913 \bullet C_3 H_8 + 1187 \bullet C_4 H_{10}. \tag{10}$$

where C_3H_8 is the propane content in the fuel, %;

C_4H_{10} is the butane content in the fuel, %.

The result of the experiment is as follows:

$$Q^d = 913 \bullet 60 + 1187 \bullet 40 = 102.26 \frac{MJ}{m^3}. \tag{11}$$

(6) Fuel and air flowrate was determined at the diaphragm due to pressure drop ΔP in the narrowed passage.

As we know from Bernoulli's equation, the flow kinetic component is determined with the following formula:

$$\Delta h = \xi \frac{w^2}{2g}, \tag{12}$$

where Δh is the pressure drop at differential manometer 14, 15 (Figure 5), m;

w is the flow velocity, m/s;

g is the acceleration of gravity, m/s^2;

ξ is the drag coefficient, which for a diaphragm with thickened edges in a straight pipe (duct) (Figure 7) is calculated with the following formula:

$$\xi_1 = \frac{\Delta P}{\rho w_1^2/2}\left[0.5 \bullet \left(1 - \frac{F_0}{F_1}\right)^{0.75} + \tau\left(1 - \frac{F_0}{F_1}\right)^{1.375} + \left(1 - \frac{F_0}{F_1}\right)^2 + \lambda\frac{l}{D_r}\right]\left(\frac{F_1}{F_0}\right)^2, \tag{13}$$

where ρ is the density of the medium flowing through the section, kg/m^3;

F is the cross-section area, m^2;

D_r is the reduced diameter, m:

$$D_r = \frac{4 \bullet F_o}{P_o}. \tag{14}$$

P_o is the section perimeter, m;

l is the diaphragm length, m;

$\acute{l}$ is the reduced diaphragm length $\acute{l} = l/D_r$, m;

λ is the adjustment factor $\lambda = 0.02$;

τ is the adjustment factor $\tau = (2.4 - \acute{l}) \bullet 10^{-\varphi(\acute{l})}$;

φ is the degree index $\varphi(\acute{l}) = 0.25 + 0.535 \bullet \acute{l}^8/(0.05\acute{l}^7)$;

Conversion of formula (12) produces equation for flow velocity w [m/s] and flow rate G [m^3/s] calculation depending on the head Δh:

$$w = \sqrt{\frac{2g \bullet \Delta h}{\xi}},$$
$$G = \frac{\pi D^2}{4} \bullet w = \frac{\pi D^2}{4} \bullet \sqrt{\frac{2g \bullet \Delta h}{\xi}}. \tag{15}$$

(7) Heat output (kW) of the combustion unit was determined according to the following formula:

$$Q = B_T \cdot Q_H^C \cdot \eta, \tag{16}$$

where B_T is the fuel consumption measured in the experiment, (m^3/s);

Q_H^C is the calorific value of the fuel, kJ/m^3;

η is the thermal efficiency of combustion in the furnace space.

(8) Heat release rate (kW/m^3) of the furnace volume was determined using the following formula:

$$\frac{Q}{V_C} = \frac{B_F \bullet Q_H^C \bullet \eta}{V_C}, \tag{17}$$

where V_C is the furnace chamber volume, m^3.

In order to determine the furnace volume V_C, half of the experimental stand volume has to be deemed actively involved in combustion. The stand has a power reserve, therefore part of its volume is not involved. We take the following stand dimensions: $0.38 \times 0.38 \times 0.7$ m.

The steam drum boilers heat release rate is usually deemed equal to 140–150 kW/m^3 for boilers designed for coal combustion. For gas-and-oil-fired boilers, the range is 200–230 kW/m^3, and for gas-tight boilers, somewhat higher [42]. Thus, the burners under consideration have heat release rates (100–142 kW/m^3) close to the standard ones for steam boiler furnaces.

3. Results

The results of experiments with propane-butane mixture combustion in the innovative swirl burner are summarized in Table 2.

The results of experiments with propane-butane mixture combustion in the cross jet gas burner are summarized in Table 3.

Upon recalculation of measured NO$_x$ and CO emissions taking into account the O$_2$ concentration in flue gases, the results were further converted into graphs. Figure 8 shows the dependences of total nitrogen oxides emissions on excess air ratio for all the given fuel consumption by both burners. Similarly, Figure 9 contains data on CO emissions depending on excess air ratio for all the given fuel consumption levels for both burners.

Figure 10 shows an overlay of nitrogen oxides and carbon monoxide emissions to determine the optimum excess air ratio interval for device no. 1. Figure 11 contains similar data for device no. 2.

The results of analysis of fuel consumption impact on NO$_x$ and CO emissions are graphically shown in Figures 12–15.

4. Discussion

Comparison of environmental performance of the two different burner devices is presented below. Upon initial examination of NO$_x$ and CO emissions dependence diagrams, it becomes obvious that stable operation of device no. 1 requires larger excess air amounts than that of device no. 2. The stable combustion range for device no. 1 is $\alpha = 1.4/2.0$ ($\varphi = 0.5/0.71$), whereas device no. 2 shows stability at $\alpha = 0.5/1.0$ ($\varphi = 1.0/2.0$). The significant difference in excess air requirements can be explained by differences in the operating principle of the burner devices. Device no. 1 needs an intensive vortex generated among other things by active air flow. Device no. 2 uses direct flows, and turbulent acceleration is created by narrowing cross-section of air flow openings rather than by air flow increase. As a result, device no. 2 operates in a lower excess air ratio interval, on average lower by 0.9.
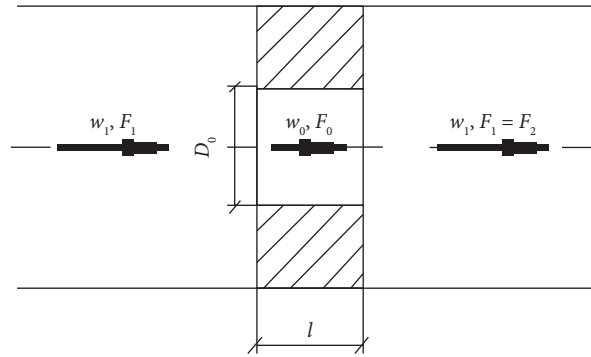
FIGURE 7: Diaphragm with thickened edges in a straight pipe (duct).

TABLE 2: Results of flue gas sampling and calculation of swirl burner technical parameters.

No.	Mass flow rate of propane-butane mixture (kg/h)	Mass air flow rate (kg/h)	α	φ	CO (ppm)	NO_x (ppm)	T_{oc} (°C)	O_2 (%)	Q/V_t (kW/m³)	Re	Q (kW)
1	0.358	7.81	1.56	0.64	1575	22.5	30.4	16.2	100.6	5809.19	3.98
2	0.358	8.21	1.64	0.61	1321	25.5	31.1	16	100.6	6093.68	3.98
3	0.358	8.59	1.71	0.58	1140	28.0	32.5	16.2	100.6	6363.94	3.98
4	0.358	8.96	1.78	0.56	1070	30.0	32.7	16.5	100.6	6627.09	3.98
5	0.358	9.31	1.85	0.54	1044	31.3	34.1	16.6	100.6	6876.01	3.98
6	0.358	9.65	1.92	0.52	1030	31.9	34	16.6	100.6	7117.83	3.98
7	0.438	8.21	1.34	0.75	978.3	24	33	14.1	123.2	6150.58	4.87
8	0.438	8.59	1.40	0.71	714.7	24.7	34	14.2	123.2	6420.84	4.87
9	0.438	8.96	1.46	0.68	620.0	25.3	34	14.1	123.2	6683.99	4.87
10	0.438	9.31	1.51	0.66	540.0	25.9	32.5	13.8	123.2	6932.91	4.87
11	0.438	9.65	1.57	0.64	477.3	27.0	26	13.6	123.2	7174.72	4.87
12	0.438	9.98	1.62	0.62	420.0	28.7	29	13.8	123.2	7409.42	4.87
13	0.438	10.29	1.67	0.60	380.0	32.3	33	13.8	123.2	7629.90	4.87
14	0.506	9.65	1.36	0.74	519.5	27.0	35.9	13.1	142.3	7223.09	5.62
15	0.506	9.98	1.41	0.71	410.1	27.8	36.1	13.1	142.3	7457.79	5.62
16	0.506	10.29	1.45	0.69	336.5	33.9	36.5	14.1	142.3	7678.26	5.62

TABLE 3: Flue gas sampling results for a gas burner with transverse jet mixing.

| No.	Mass flow rate of propane-butane mixture (kg/h)	Mass air flow rate (kg/h)	α	φ	CO (ppm)	NO_x (ppm)	T_{oc} (°C)	O_2 (%)	Q/V_t, (kW/m³)	Re	Q (kW)
1	0.358	3.1	0.62	1.61	27.45	45.5	22.7	12.5	100.6	1728.51	4.02
2	0.358	3.58	0.71	1.41	25.00	60.0	22.3	15.6	100.6	1968.44	4.02
3	0.358	4.01	0.80	1.25	24.00	65.0	22.3	15.3	100.6	2183.38	4.02
4	0.358	4.39	0.87	1.15	23.18	66.1	22.3	15.7	100.6	2373.32	4.02
5	0.358	4.74	0.94	1.06	22.42	66.5	22.4	15.5	100.6	2548.27	4.02
6	0.438	3.1	0.50	2.00	170.8	39	21.4	13.2	123.2	1768.50	4.92
7	0.438	3.58	0.58	1.72	71.05	45.2	21.7	13.4	123.2	2008.43	4.92
8	0.438	4.01	0.65	1.54	40.08	48.2	21.8	13.5	123.2	2223.37	4.92
9	0.438	4.39	0.71	1.41	30.00	49.8	22.2	13.5	123.2	2413.31	4.92
10	0.438	4.74	0.77	1.30	26.00	50.9	22.3	13.2	123.2	2588.26	4.92
11	0.438	5.07	0.82	1.22	24.00	51.5	22.2	13.9	123.2	2753.21	4.92
12	0.438	7.39	1.20	0.83	17.00	52.3	23.7	13.0	123.2	3912.88	4.92
13	0.438	8.21	1.34	0.75	15.00	53.0	23.6	13.9	123.2	4322.77	4.92
14	0.438	8.96	1.46	0.68	13.00	54.9	23.6	14.4	123.2	4697.66	4.92
15	0.506	3.58	0.50	2.00	177.1	39.2	22.3	12.3	142.3	2042.42	5.69
16	0.506	4.01	0.56	1.79	67.19	43.8	22.6	12.3	142.3	2257.36	5.69
17	0.506	4.39	0.62	1.61	40.00	45.0	22.5	12.4	142.3	2447.30	5.69
18	0.506	4.74	0.67	1.49	27.45	45.4	22.7	12.5	142.3	2622.25	5.69
19	0.506	5.07	0.71	1.41	21.12	45.5	22.3	13.2	142.3	2787.21	5.69
20	0.506	5.38	0.76	1.32	18.00	45.5	22.7	12.5	142.3	2942.16	5.69
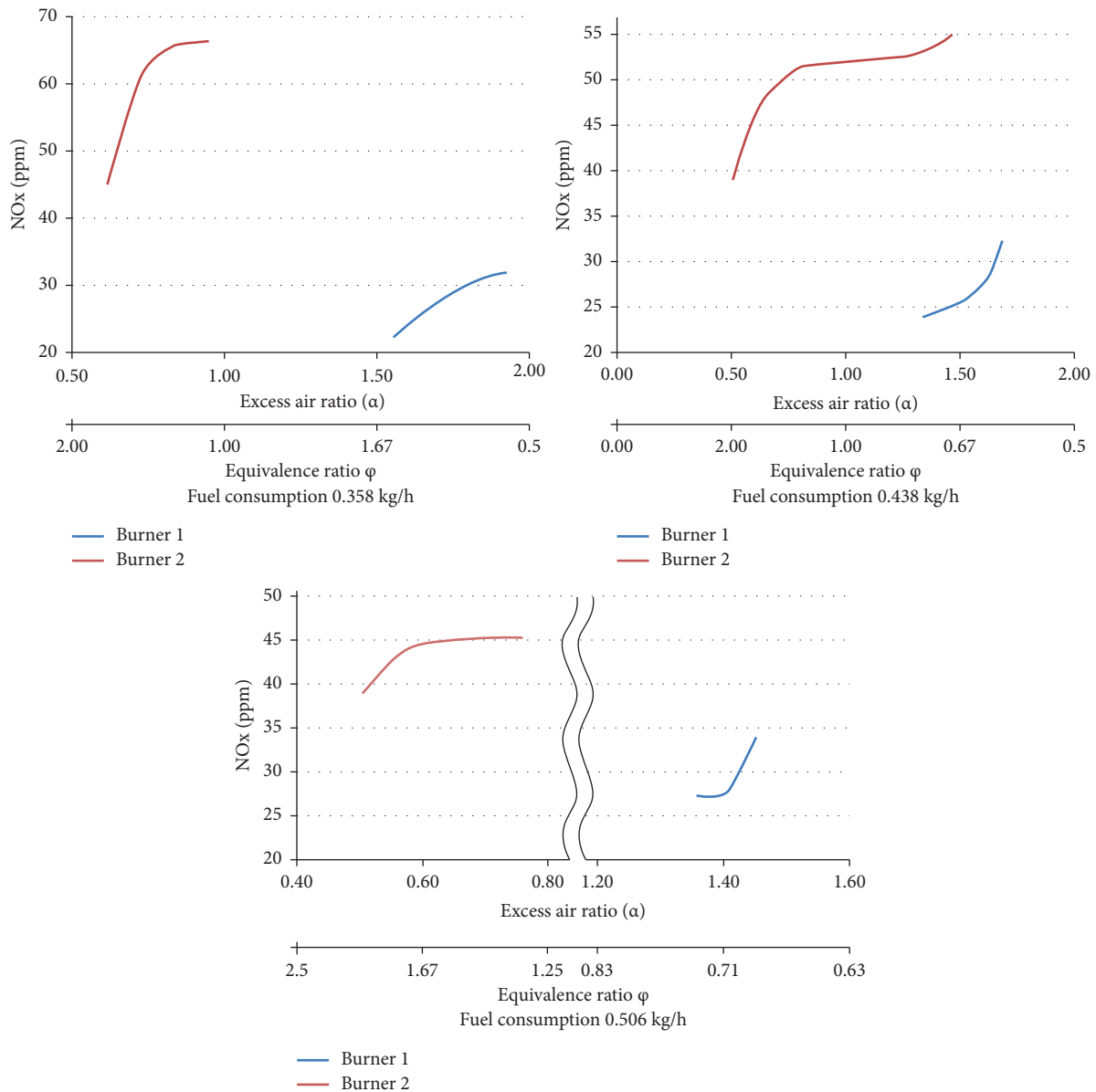
FIGURE 8: Dependence of total NO_x emissions on excess air ratio for fuel consumption levels 0.358 kg/h, 0.438 kg/h, and 0.506 kg/h.

In terms of total nitrogen oxides in Figure 8, device no. 1 is superior to device no. 2. The NO_x values are on average between 25 and 35 ppm (device no. 1). However, device no. 2 values are between 40 and 65 ppm, on average 1.75 times the NO_x values of device no. 1. The difference is achieved through abundant dilution of combustion products with conditionally cold air in device no. 1, which reduces the overall temperature level and the intensity of thermal nitrogen oxides formation. It should be noted that device no. 1 does not exceed worldwide requirements to nitrogen oxide emission levels. In addition, active air flow breaks up local zones of increased fuel concentration and temperature. It leads to uniform distribution of heat in the combustion chamber.

As expected, the CO levels (Figure 9) are inversely related to NO_x. The average carbon monoxide emissions by both units are strongly dependent on fuel consumption. Device no. 2 generates nitrogen monoxide emissions in the range of 20/160 ppm. Device no. 1 significantly exceeds these figures, 350/1600 ppm, thus reaching 10 times higher emission levels than device no. 2. The significant CO excess in device no. 1 demonstrates the obvious fuel underburning. Combustion is incomplete due to unacceptably small dimensions of the swirl burner (device no. 1) insufficient for intense swirl generation at the given fuel flow rate. The flow of fuel-air mixture entering the chamber does not have enough time to swirl and bursts into the outlet nozzle taking unburned fuel with it. Device no. 1 has limitations in terms
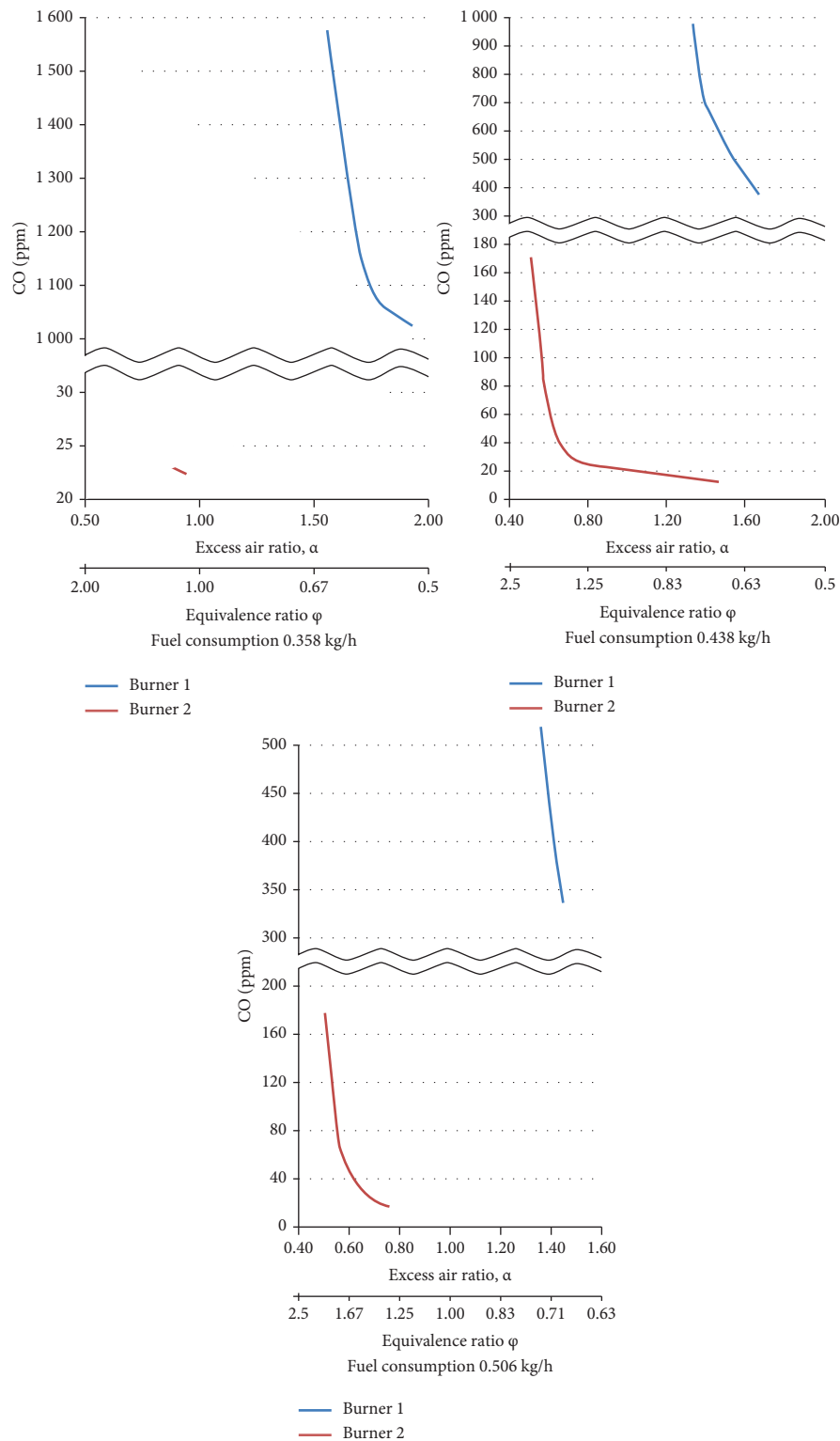
FIGURE 9: Carbon monoxide (CO) emissions by swirl burner 1 and cross jet burner 2.

of minimum dimensions and consequently minimum fuel consumption. The obvious solution is that the device must have larger dimensions, similar to prototype [33].

Analysis of dependencies in Figure 10 shows that an optimum range of excess air values for Device no. 1 exists.

The average value α decreases as fuel consumption increases, as shown in Figure 16. A regression relationship with polynomial degree 2 was obtained for this curve, allowing calculation of α with average relative deviation error $3.4 \cdot 10^{-4}$%:
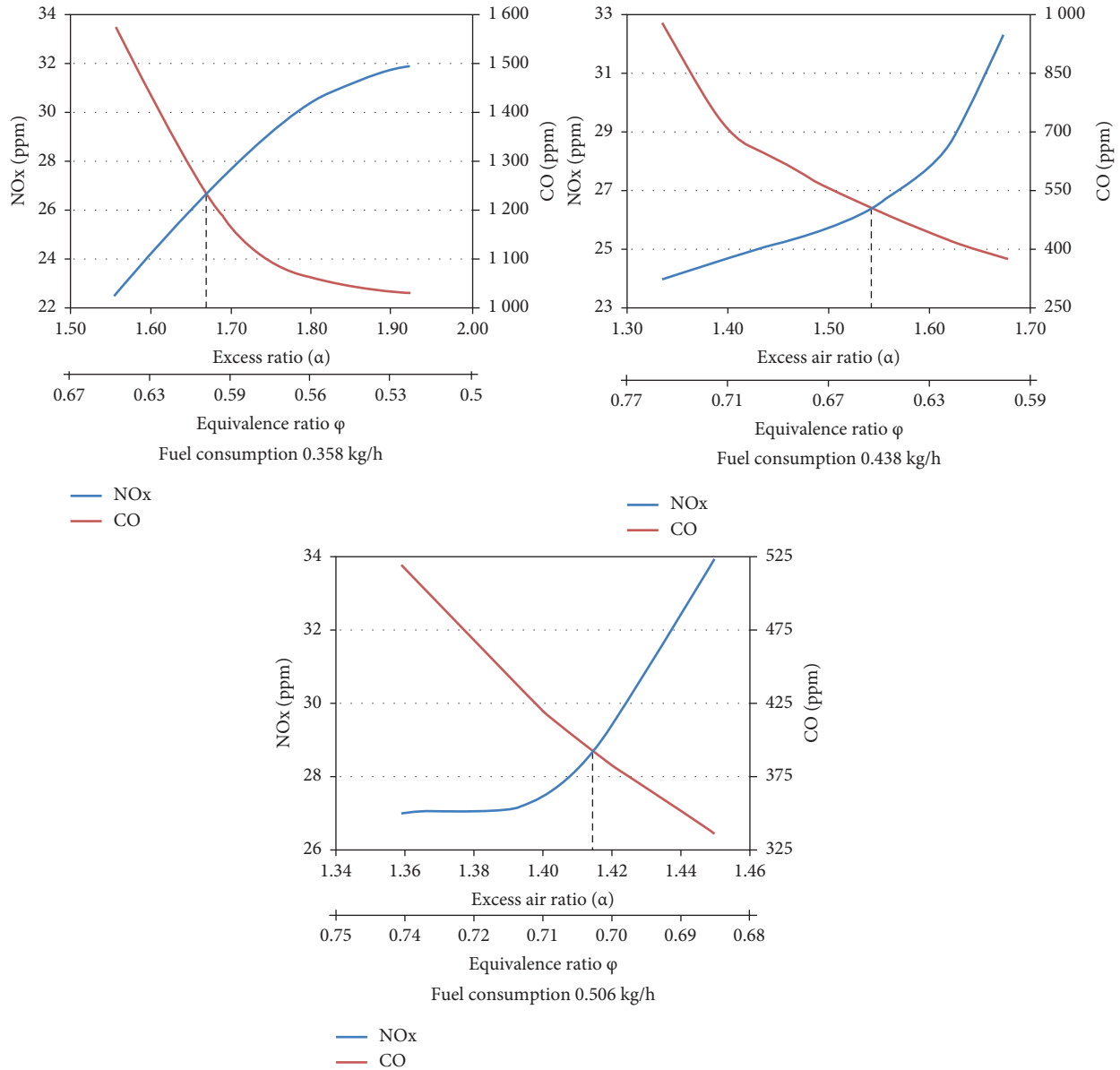
FIGURE 10: Dependence of total NO_x and CO emissions on excess air ratio, fuel consumption 0.358 kg/h, 0.438 kg/h, and 0.506 kg/h for swirl burner device no. 1.

$$\alpha = 2.0484972 - 0.420892 \cdot B_F - 1.086882 \cdot B_F^2, \qquad (18)$$

where B_F is the fuel consumption, kg/h.

Equation (18) allows us to calculate the excess air ratio for device no. 1 and any fuel consumption with high degree of accuracy.

Figure 11 also confirms that, in device no. 2, excess air ratio decreases as fuel consumption goes up. The dependence of excess air ratio α on fuel consumption for cross jet burner is graphically shown in Figure 17. Regression equation (19) allows us to calculate α with average relative deviation error of 0.057% for any fuel consumption B_F, kg/h:

$$\alpha = \frac{B_F}{-0.60671 + 2.8739 \cdot B_F}. \qquad (19)$$

The regression equations (18) and (19) were obtained by the least squares method.

Figures 12–15 provide an estimate of the fuel consumption effect on emission levels. Figure 12 shows that, in device no. 1, an increase in fuel consumption does not significantly change NO_x emissions having a greater impact on the required excess air ratio. In case of device no. 2 (Figure 13), the relationship between NO_x and fuel consumption is more pronounced: the amount of NO_x goes
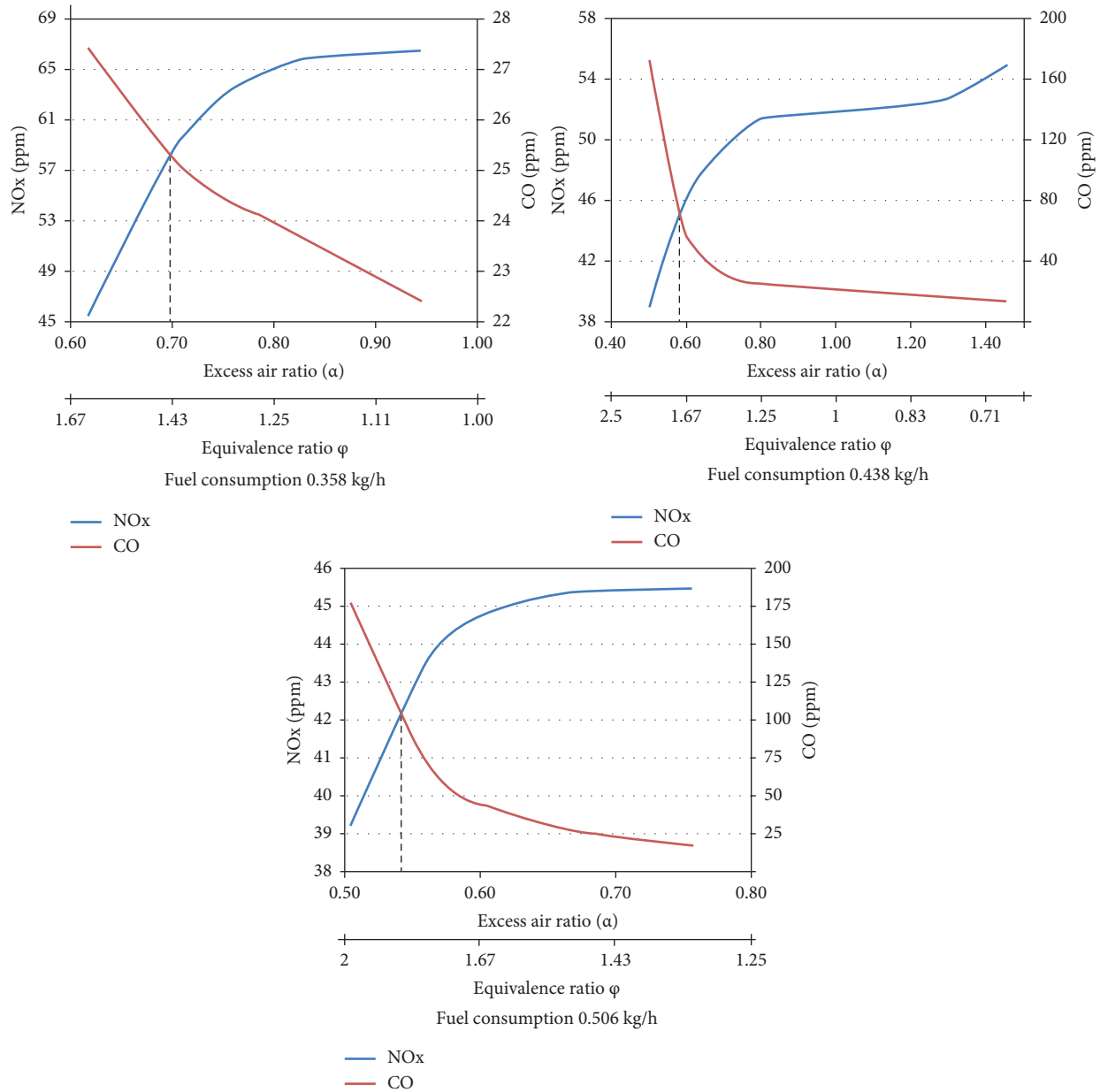
FIGURE 11: Dependence of total nitrogen oxide NO$_x$ and carbon monoxide CO emissions on excess air ratio, fuel consumption 0.358 kg/h, 0.438 kg/h, and 0.506 kg/h for cross jet burner device no. 2.

down as fuel consumption grows, while the fuel consumption impact on air ratio is negligible. More fuel evenly fills the furnace volume preventing formation of local high temperature zones and reducing nitrogen oxides output.

Carbon monoxide emissions in device no. 1 are obviously reduced as fuel consumption increases (Figure 14). Larger amounts of fuel are forced to stay in the burner vortex for longer periods of time and burn out more intensively. At
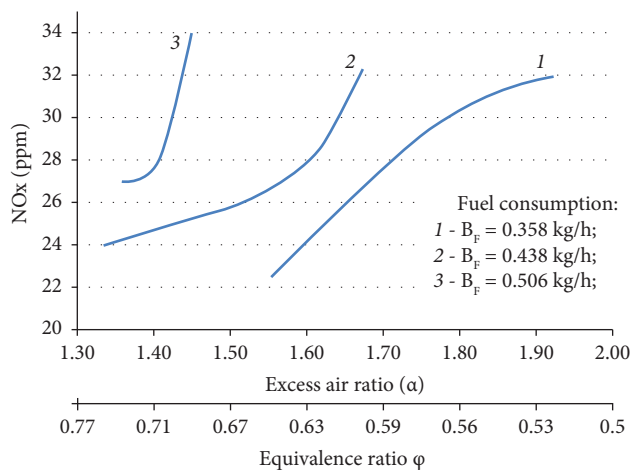
Figure 12: Dependence of total NO_x emissions on excess air ratio for different fuel consumption levels in the swirl burner device no. 1.
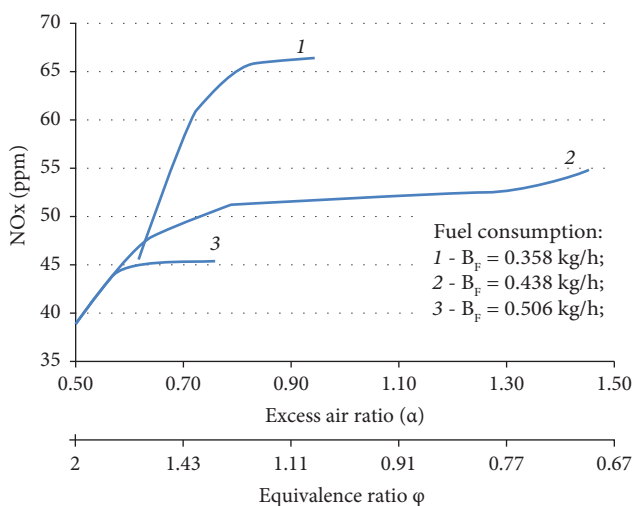
Figure 13: Dependence of total NO_x emissions on excess air ratio for different fuel consumption levels in the cross jet burner device no. 2.
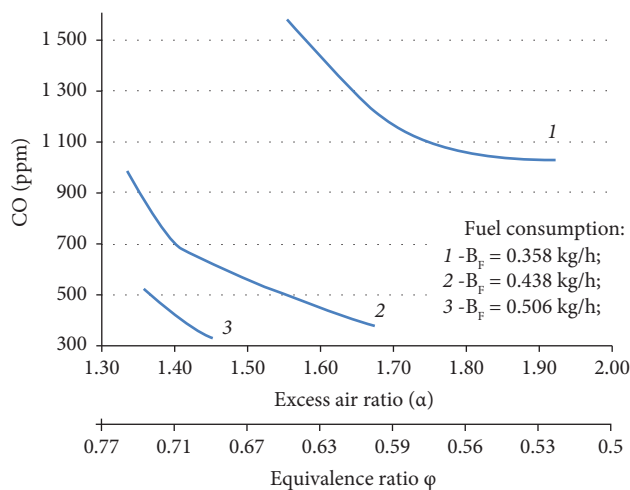
Figure 14: Dependence of carbon monoxide CO emissions on excess air ratio for different fuel consumption levels in the swirl burner device no. 1.
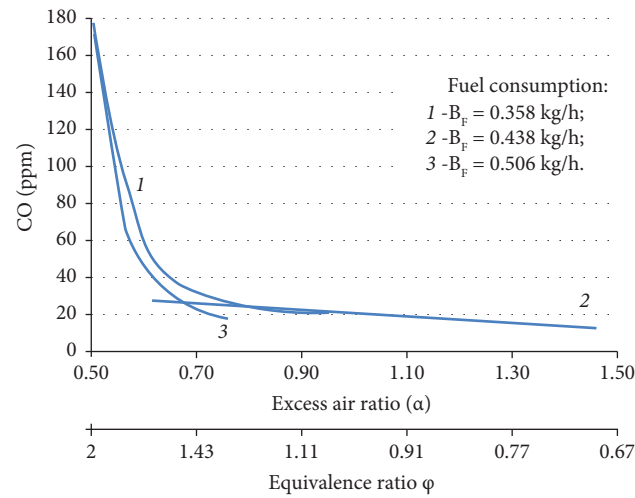
FIGURE 15: Dependence of carbon monoxide CO emissions on excess air ratio for different fuel consumption levels in a cross jet burner device no. 2.
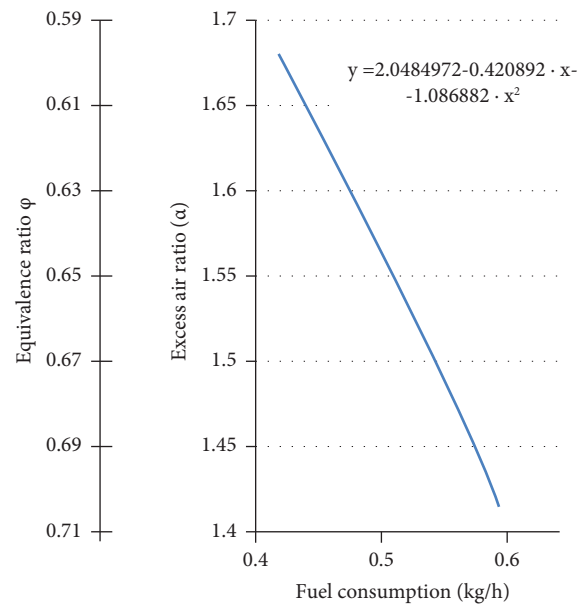

FIGURE 16: Dependence of excess air ratio α on fuel consumption for swirl burner device no. 1.
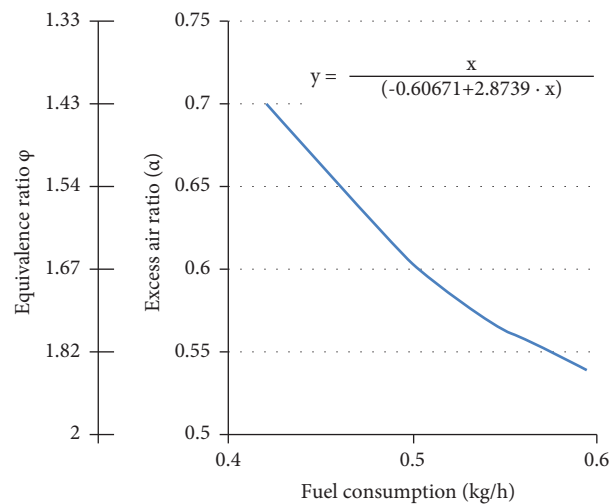

FIGURE 17: Dependence of excess air ratio on fuel consumption for cross jet burner device no. 2.

the same time, an increase in fuel consumption brings down the required excess air ratio.

Figure 15 demonstrates the fact that, in device no. 2, the CO emissions are almost independent of the fuel consumption level (curves are merged). The only impact factor in this case is excess air ratio. As excess air ratio increases, the CO emissions decrease.

5. Conclusion

Comparison of two fundamentally different burner designs for combustion of small volumes of combustible gas has showed that

(1) in terms of NO_x emissions, the swirl burner is superior to the cross jet burner with a 1.75-fold difference in total nitrogen oxides

(2) in terms of carbon monoxide (CO) emissions, the cross jet burner is 10 times more efficient than the swirl burner

The cross jet burner was originally manufactured as laboratory equipment and its dimensions as well as combustion air flow rate were selected in strict compliance with the expected lowest emission levels. During the experiment, a considerable advantage of the device over the swirl burner was observed in terms of CO emissions. This is due to the fact that ultrasmall dimensions of the swirl burner fail to ensure sufficient vortex formation inside the chamber and promote direct outflow of unburned mixture, although the basic idea behind the swirl burner design is to organize the vortex inside in order to keep the mixture in the reaction zone. This problem can be successfully solved by increasing the size and consequently the output of the swirl burner. Device no. 2 must be at least twice as large in size and performance. The test results for a larger device are not discussed in this paper.

Comparison of NO_x produced by the two burners leads to the conclusion that the flow swirling according to the "tornado" principle in the swirl burner significantly reduces emissions (by 80–90%) due to a longer stay of the fuel-air mixture in the combustion chamber promoting the atomic nitrogen reduction reactions. In addition, the process of combustion products dissolution in excess air has a significant impact. The stable combustion range for device no. 1 is $\alpha = 1.4/2.0$ ($\varphi = 0.5/0.71$), whereas device no. 2 shows stability at $\alpha = 0.5/1.0$ ($\varphi = 1.0/2.0$). The excess air is drawn in from the space around and is not heated intentionally to have an ambient temperature. As a result, the overall temperature level at the flare core is reduced having a positive effect on nitrogen oxides formation. The excess air ratio in swirl burner 1 is on average 0.9 times higher than that in cross jet burner 2. Nitrogen dioxide formation is generally more sensitive to temperature than nitrogen monoxide formation.

As a result of the experiment, it was proved that the swirl burner previously used only for combustion of liquid fuels, both traditional and alternative, can effectively compete with specialized burners operating exclusively on gas. The minimum output limitations of this burner must be taken into account.

The experiment also highlighted the need to develop a larger swirl burner prototype to achieve the most efficient swirl within the device and burn the fuel-air mixture more completely while maintaining high efficiency and flexibility to operate on different types of fuel without major design changes.

Despite the relatively small dimensions of both units, in the vortex burner device, as compared to its peer, fuel and air input can be changed to a larger extent while stable combustion without flame failure is maintained. In case of the cross jet burner, air supply could not exceed 8.46 kg/h, as at higher levels, the flame became unstable and fluctuation of most indicators increased. The steadier operation of device no. 1 with higher fuel-air mixture consumption made it possible to achieve higher output, higher heat release rate of 142 kW/m^3 as compared to device no. 2 with the value of 100 kW/m^3.

The main conclusion is that swirl burner 1 can be widely used in the power sector with a minimum output limit. The cross jet burner 2 is also widely applicable in the industry despite being limited to gaseous fuel alone. Therefore, the choice of device will depend on external factors: type of fuel, problems that have to be solved, etc.

Data Availability

The data used to support the finding of the study are included in the paper.

Conflicts of Interest

The authors declare that they have no conflicts of interest.

References

[1] Ns 28775-90, *Gas turbine driven gas compressor units. General Specifications*, Moscow: Standard Inform, Moscow, Russia, 2005.

[2] A. H. Lefebvre, *Gas Turbine Combustion: Alternative Fuels and Emissions*, CRC Press, Boca Raton, FL, USA, 2010.

[3] Usepa Federal Register, "Review of national ambient air quality standards for carbon monoxide," *Final Rule. Rules and Regulations*, vol. 76, no. 169, 2011.

[4] Eur-Lex home, "Directive 2010/75/EU of the European Parliament and of the Council of 24 November 2010 on industrial emissions (integrated pollution prevention and control)," *Official Journal of the European Union*, vol. 15.

[5] D. Wen-jiao, L. Jian-lei, C. Shui-yuan, J. Jia, and W. Xiao-qi, "Air pollutant emission inventory from iron and steel industry in the Beijing tianjin-hebei region and its impact on $PM_{2.5}$," *Environmental science*, vol. 39, no. 4, pp. 1445–1454, 2018.

[6] G. N. Abramovich, T. A. Girshovich, S. Y. Krasheninikov, A. N. Sekundov, and I. P. Smirnova, *Turbulent Jet Theory*, G. N. Abramovich, Ed., Moscow: Science. Main editorial board for physical and mathematical literature, Moscow, Russia, 2 edition, 1984.

[7] R. B. Akhmedov, *Aerodynamics of Swirling Jets*, Energia, Soviet Union, 1977.

[8] A. M. Dostiyarov and S. B. Sadykova, "Micro-Modular air driven combustion nozzle: experimental and numerical

modelling studies towards optimal geometric design," *Thermal Science*, vol. 26, no. 2 Part B, pp. 1557–1566, 2022.

[9] A. Renaud, S. Ducruix, and L. Zimmer, "Experimental study of the precessing vortex core impact on the liquid fuel spray in a gas turbine model combustor," *Journal of Engineering for Gas Turbines and Power*, vol. 141, no. 11, 2019.

[10] R. R. Tacina, "Low NOx potential of gas turbine engines," *AIAA Aerospace Sciences Meeting and Exhibit*, vol. 90, 1990.

[11] A. H. Lefebvre, "The role of fuel preparation in low-emission combustion," *Journal of Engineering for Gas Turbines and Power*, vol. 117, no. 4, pp. 617–654, 1995.

[12] M. J. Moore, "NOₓ emission control in gas turbines for combined cycle gas turbine plant," *Proceedings of the Institution of Mechanical Engineers, Part A: Journal of Power and Energy*, vol. 211, no. 1, pp. 43–52, 1997.

[13] J. Fritz, M. Kro¨ner, and T. Sattelmayer, "Flashback in a swirl burner with cylindrical premixing zone," *Journal of Engineering for Gas Turbines and Power*, vol. 126, no. 2, pp. 276–283, 2004.

[14] Y. Sommerer, D. Galley, T. Poinsot, S. Ducruix, F. Lacas, and D. Veynante, "Large eddy simulation and experimental study of flashback and blow-off in a lean partially premixed swirled burner," *Journal of Turbulence*, vol. 5, 2004.

[15] D. Galley, S. Ducruix, F. Lacas, and D. Veynante, "Mixing and stabilization study of a partially premixed swirling flame using laser induced fluorescence," *Combustion and Flame*, vol. 158, no. 1, pp. 155–171, 2011.

[16] S. Candel, "Combustion dynamics and control: progress and challenges," *Proceedings of the Combustion Institute*, vol. 29, no. 1, pp. 1–28, 2002.

[17] T. C. Lieuwen and V. Yang, "Combustion instabilities in gas turbine engines(operational experience, fundamental mechanisms and modeling)," *Progress in Astronautics and Aeronautics*, American Institute of Aeronautics and Astronautics, Reston, VI, USA, 2005.

[18] S. Wood and A. T. Harris, "Porous burner for lean-burn applications," *Progress in Energy and Combustion Science*, vol. 34, Article ID 667e84, 2008.

[19] Y. Yu, W. Gaofeng, L. Qizhao, M. Chengbiao, and X. Xianjun, "Flameless combustion for hydrogen containing fuels," *International Journal of Hydrogen Energy*, vol. 35, no. 7, pp. 2694–2697, 2010.

[20] M. Jianchun, L. Pengfei, and Z. Chuguang, "Numerical simulation of flameless premixed combustion with an annular nozzle in a recuperative furnace," *Chinese Journal of Chemical Engineering*, vol. 18-1, pp. 10–17, 2010.

[21] G. Ting-ting and L. andShao-hua, "Numerical simulation of turbulent jets with lateral injection into a cross flow," *Journal of Hydrodynamics*, vol. 18-3, pp. 319–323, 2006.

[22] J. Fritz, M. Kröner, and T. Sattelmayer, "Flashback in a swirl burner with cylindrical premixing zone," *Journal of Engineering for Gas Turbines and Power*, vol. 126, no. 2, pp. 276–283, 2004.

[23] M. Konle and T. Sattelmayer, "Interaction of heat release and vortex breakdown during flame flashback driven by combustion induced vortex breakdown," *Experiments in Fluids*, vol. 47, no. 4-5, pp. 627–635, 2009.

[24] T. Sattelmayer, C. Mayer, and J. Sangl, "Interaction of flame flashback mechanisms in premixed hydrogen-air swirl flames," *Journal of Engineering for Gas Turbines and Power*, vol. 138, no. 1, Article ID 011503, 2016.

[25] A. E. Khalil and A. K. Gupta, "Velocity and turbulence effects on high intensity distributed combustion," *Applied Energy*, vol. 125, pp. 1–9, 2014.

[26] K. I. Khidr, Y. A. Eldrainy, and M. M. El-Kassaby, "Towards lower gas turbine emissions: flameless distributed combustion," *Renewable and Sustainable Energy Reviews*, vol. 67, pp. 1237–1266, 2017.

[27] Y. Tu, S. Xu, M. Xie, Z. Wang, and H. Liu, "Numerical simulation of propane MILD combustion in a lab-scale cylindrical furnace," *Fuel*, vol. 290, Article ID 119858, 2021.

[28] G. Sorrentino, P. Sabia, P. Bozza, R. Ragucci, and M. de Joannon, "Impact of external operating parameters on the performance of a cyclonic burner with high level of internal recirculation under MILD Combustion conditions," *Energy*, vol. 137, pp. 1167–1174, 2017.

[29] T. G. Reichel, S. Terhaar, and O. Paschereit, "Increasing flashback resistance in lean premixed swirl-stabilized hydrogen combustion by axial air injection," *Journal of Engineering for Gas Turbines & Power*, vol. 137, no. 7, Article ID 071503, 2015.

[30] Q. Xu, Z. Zou, Y. Chen et al., "Performance of a novel-type of heat flue in a coke oven based on high-temperature and low-oxygen diffusion combustion technology," *Fuel*, vol. 267, Article ID 117160, 2020.

[31] Q. Xu, K. Wang, J. Feng et al., "Performance analysis of novel flue gas self-circulated burner based on low-NOx combustion," *Journal of Energy Engineering*, vol. 146, no. 2, Article ID 04019041, 2020.

[32] Q. Xu, M. Shen, K. Xie et al., "Heat and mass transfer mechanism and control strategy of clean low carbon combustion technology in the novel-type coke oven flue with MILD combustion," *Fuel*, vol. 320, Article ID 124001, 2022.

[33] A. Baubek, A. Atyaksheva, M. Zhumagulov, N. Karjanov, I. Plotnikova, and N. Chicherina, "Complex studies of the innovative vortex burner device with optimization of design// studies in systems," *Decision and Control*, vol. 351, pp. 139–153, 2021.

[34] S. B. Sadykova, A. M. Dostiyarov, M. G. Zhumagulov, and N. R. Kartjanov, "Influence of turbulence on the efficiency and reliability of combustion chamber of the gas turbine," *Thermal Science*, vol. 25, no. 6, pp. 4321–4332, 2021.

[35] A. Baubek, M. Zhumagulov, N. Kartjanov, S. Sadykova, and M. Arpabekov, "Experimental test of water-oil emulsion combustion," *E3S Web of Conferences*, vol. 178, Article ID 01012, 2020.

[36] A. A. Baubek, M. G. Zhumagulov, M. V. Dolgov, and N. R. Kartjanov, "Combustion device for hydrocarbon fuel," Patent of the Republic of Kazakhstan No. 35578, 2022.

[37] A. M. Gribkov, A. A. Baubek, M. G. Zhumagulov, S. A. Glazyrin, and M. V. Dolgov, "Swirl burner device," Patent of the Russian Federation No. 2769048, 2022.

[38] J. M. Gerald, "Low NO$_{\text{sub.x}}$ cyclone furnace steam generator," Babcock & Wilcox Power Generation Group, Inc, Patent 7,926,432 B2, 2011.

[39] V. P. Preobrazhensky, *Measurements and Instrumentation in Heat Engineering*, vol. 1 & 2, Mir Publishers, Moscow, Russia, 1980.

[40] Ingeneryi.Info, "Millivoltmeter MR-64-02," https://ingeneryi.info/elektronika-elektrika/ne-razobrannoe-elektrika/2545-millivoltmetr-mr-64-02.html.

[41] cleanaireurope.com, "Testo 350 M/XL short operation instruction manual," https://cleanaireurope.com/wp-content/uploads/2020/06/Manual-Testo-350-XL.pdf.

[42] N. V. Kuznetsov and V. V. Mitor, *Thermal Calculation of Boiler Units*, Normative Method, Energia, Soviet Union, 1973.